# The effect of citric acid and selenization onto electrochemically deposited Copper-Indium thin films for solar cell applications

Ashwini B. Rohom, Priyanka U. Londhe, Nandu B. Chaure

PII: S0040-6090(17)30740-X
DOI: doi:10.1016/j.tsf.2017.09.057
Reference: TSF 36265

To appear in: *Thin Solid Films*

Received date: 23 December 2016
Revised date: 19 September 2017
Accepted date: 29 September 2017

Please cite this article as: Ashwini B. Rohom, Priyanka U. Londhe, Nandu B. Chaure , The effect of citric acid and selenization onto electrochemically deposited Copper-Indium thin films for solar cell applications. The address for the corresponding author was captured as affiliation for all authors. Please check if appropriate. Tsf(2017), doi:10.1016/j.tsf.2017.09.057

# The effect of citric acid and selenization onto electrochemically deposited Copper-Indiun thin films for solar cell apllications

Ashwini B. Rohom, Priyanka U. Londhe and Nandu B. Chaure**
Electrochemical Laboratory, Department of Physics, Savitribai Phule Pune University,
(formerly University of Pune) Pune 411007, India
*Email - n.chaure@physics.unipune.ac.in

## Abstract

Copper Indium diselenide (CISe) layers have been synthesized via two stage processes; electrodeposition of Copper-Indium (Cu-In) and selenization. The effect of complexing agent, citric acid (CA) was studied on the growth of Cu, In and Cu-In layers. Polycrystalline Cu-In layers were electrodeposited from aqueous bath at -0.85V versus Ag/AgCl reference electrode. The structural, optical, morphological, compositional, photoelctrochemical and optoelectronic properties for Cu-In layer and selenized Cu-In layers are studied. Three prominent reflections of tetragonal crystal structure of CISe, (112), (204/220) and (312/116) were exhibited in selenized layers. Nearly uniform, void-free surface morphology was observed in selenized samples. Upon selenization of Cu-In layers prepared with 0.1 M CA produced stoichiometric CISe thin films. The energy band-gap values are estimated between 1.05 eV to 1.18 eV. Photoelectrochemical cell measurement revealed the growth of p-type and n-type conductivity of CISe thin films. The peaks related to chalcopyrite CISe and ordered defect compound are observed in Raman analyses. The superstrate solar cell structure prepared with selenized Cu-In layer deposited in presence of 0.1 M CA measured 4.05% efficiency. . The values of $R_s$, 7.42 $\Omega$-cm$^2$, 0.94 $\Omega$-cm$^2$ and G, 1.01 mS/cm$^2$ 10.25 mS/cm$^2$ were calculated under dark and illuminated condition, respectively. We believe that the measured efficiency is low; however the further improvement is possible by optimizing the surface treatment conditions.

Keywords: *Cu-In alloy, copper indium diselenide, Electrodeposition, Thin film Solar cells, Selenization*

## INTRODUCTION

Ternary and quaternary based chalcogenides have been attracted tremendous scientific and technological interest towards the development of thin film solar cell because of its high absorption coefficient and long mean free path of the charge carriers [1-2]. From chalcogenide family CISe based materials are widely used as absorber for photovoltaic application since its direct band gap can be tailored from 1.04 eV to 1.68 eV upon the addition of sulfur and/or gallium [3-4]. Several methods have been employed for the deposition of $CuInS_2$ (CIS) and CISe such as molecular beam epitaxy [5], physical vapor deposition [6], spray pyrolysis [7], sputtering [8-9], chemical bath deposition [10], electrodeposition [11] etc. The highest efficiency of $CuInGaSe_2$ based solar cell ~ 22.3% has been reported using the co-evaporation method [12]. The major limitations of physical technique are slow deposition rate, high purity expensive targets, initial capital investment, etc. Electrodeposition (ED) is one of the low-cost techniques, with numerous advantages such as, negligible waste of chemicals, high deposition rate and deposition over large area with controlled stoichiometry [13-15]. The co-deposition of Cu-In-Se is rather complex due to different chemical and electrochemical behavior of each element. In general, CIS, CISe layers are electrodeposited by two individual processes viz, co-deposition of all elements in single bath and selenization or sulphurization of Cu-In layer. Bhattacharya et al [16] has reported 15.4% conversion efficiency by electrodeposition in conjunction with the PVD technique to adjust the content of Ga. Recently, Lee et al (17) have reported 10.01% efficiency for CISe thin film solar cells prepared by ED technique. The difficulty with single step co-deposition is to achieve the desired stoichiometry due the wide differences in the redox potentials of Cu, In, Ga and Se. Excessive copper selenide phases in CISe/CIGSe are highly conductive, which may produce shunt paths and could be destructive to efficiency of solar cell. This problem can be resolved by using complexing agents such as, citric acid (CA) [18], triethanolamine [19], EDTA [20], ethylene diamine [21], thiocynate [22], however, large amount of complexing agent is the source of impurities. Furthermore, the unwanted binary or metallic phases might be formed upon the post-deposition heat treatment which directly affect on solar cell performance. To overcome these issues, we have prepared Cu-In alloy layer by electrodeposition technique in presence of comparatively low quantity of citric acid and selenized in tubular furnace. The electrodeposition of bimetallic Cu-In alloys from single bath is reported in the literature [23-25]. Pottier et al. [26] documented the electrodeposition of CISe in acidic solution containing CA as complexing agent. Thouin et al. also used the CA as complexing agent of CISe and observed the improvement in crystallinity and adhesion of the film [27]. Luo et. al

[28] deposited Cu-In layers by pulsed laser deposition, with the formation of $Cu_{11}In_9$ phase along with metallic In. The deposition of elemental Cu or In is disadvantageous, which leads to the formation of binary phases with selenization. Prosini et al. reported the electrodeposition of Cu-In layers with studies on the effect of substrate surface treatment on the nucleation mechanism of Cu-In layers [29]. Herrero et al. studied the electrodeposition of Cu-In layer in CA on to Ti substrate and subsequent annealing in sulfur atmosphere to form $CuInS_2$ [30]. Rotating disc electrodeposition was used by Cummings et al. to prepare Cu-In layers and used subsequent selenization to produce CISe [31].

Nanoparticles of Cu-In have been prepared by Liu et al. [32] and selenized for the formation of CISe. Norswaorthy et al, synthesized micrometer sized Cu-In particles using melt atomization technique with 10.5 % solar cell conversion efficiency [33]. Kind et al, synthesized citrate capped $Cu_{11}In_9$ nanoparticles by polyol method with solar cell with efficiency 7 % [34].

We report the growth of well adherent, stoichiometric Cu-In alloy thin film by electrochemical technique as well as CISe thin film upon controlled selenization. Furthermore, n and p-type conductivity CISe layers are grown and used them on the development of superstrate solar cell structure (glass/FTO/CdS/CISe/Au) and reported over 4 % efficient thin film solar cells.

## 2.0 EXPERIMENTAL DETAILS

### *2.1 Chemicals*

All chemicals used for the synthesis of Cu-In thin film were purchased from Sigma-Aldrich of purity at least 99.9%. Fluorine doped tin oxide (FTO) coated glass substrates of sheet resistance 10-15 Ω/□ were purchased from Pilkington glass company, UK. The double distilled deionized water was used as a solvent.

### *2.2 Electrodeposition of Cu-In thin film*

Copper chloride ($CuCl_2$) and Indium chloride ($InCl_3$), were used as ionic sources of Cu and In. A standard three-electrode geometry consisting FTO, Ag/AgCl and graphite were used as working, reference and counter electrode, respectively. CA was used as a complexing agent. The cyclic voltammograms are recorded without agitation at 45 $^{o}$C (±1 $^{o}$C) with scan rate 5 mV sec$^{-1}$. Cu-In layers were electrodeposited at -0.85 V versus Ag/AgCl in presence of 0.1 M, 0.3 M and 0.5 M concentrations of CA for 60 minutes. Immediately after deposition the samples were thoroughly rinsed in ultrasonic bath with warm water and dried in laboratory atmosphere. The samples were selenized in a selenization chamber at 400 $^0$C for 20 minutes.

### *2.3 Materials characterization*

Cyclic voltammetry measurements were performed using Biologic potentiostat/galvanostat, SP-150. The structural properties were studied by means of X-ray diffractometer, (Bruker D8) with Cu K$\alpha$ anode having wavelength 0.154 nm. Optical absorption measurements were performed with JASCO UV-vis-NIR spectrometer. Surface topography was recorded with the aid of scanning electron microscope (JEOL JSM 6360A) with an operating voltage 20 kV and probe current 1 nA. The elemental atomic percentage concentration was determined by energy dispersive x-ray analysis (EDAX) technique. The Potentiostat, SP 150, Biologic equipped with two probe measurement setup was employed to study the electrical (*I-V*) properties. The conductivity type of selenized Cu-In (CISe) layers was obtained by photoelectrochemical (PEC) analysis. Three-electrode geometry was employed for PEC studies with graphite and Ag/AgCl as counter and reference electrode, respectively in 1 M KCl solution. Bias potential 10 mV was applied and the experiment was performed under white light source of intensity 10 mW/cm$^2$. The area working and counter electrode was kept constant for all samples 0.35 cm$^2$ and 2 cm$^2$. Raman analysis was performed by INVIA Renishaw micro Raman spectrophotometer with 785 nm excitation laser. A layer of Cu-In utilized for the development of solar cell was electrodeposited at -0.85 V with 0.1 M CA. CdS films of thickness ~ 70 to 100 nm were deposited by chemical bath deposition technique [35]. Prior to metal contacts CdS/selenized Cu-In layers were etched in sodium cyanide (NaCN) solution to remove the unwanted secondary phases formed during the selenization process. The final solar cell device was measured under illumination with 100 mW/cm$^2$ at room temperature.

## 3.0 RESULTS AND DISCUSSION

### *3.1 Cyclic voltammetry*

Electrochemical behavior of Cu and In was studied for various concentrations of CA. Figure 1 depicts the cyclic voltammograms (CV) $CuCl_2$ on FTO coated glass substrate. Two small shoulders revealed in the cyclic voltammogram (CV) obtained without CA (figure 1 a) about -0.11 V and -0.31 V are associated to the reduction of $Cu^{2+}$ to Cu [36,37] by equation (1). Figure (b-d) represents the CV's for $CuCl_2$ solution in presence of 0.1 M to 0.5 M CA. The onset of reduction peak was found to be shifted to higher cathodic potentials with the addition of CA from -0.11 V to -0.34 V and -0.31 V to -0.56 V probably due to change in open circuit potential indicates the complex formation of $Cu^{2+}$ with CA, which reduces the $Cu^{2+}$ activity. The origin of the earlier shoulder is not clear, which could be probably due to under-potential reduction of $Cu^{2+}$ to Cu.

$$Cu^{2+} + 2e^{-} \rightarrow Cu \qquad E_0 = +0.340 \text{ V versus NHE} \qquad \text{----------} \ (1)$$

The peak observed during anodic scan around +0.2 to +0.3 V could be related to the oxidation of Cu. A similar experiment was performed for an electrolyte containing 6 mM $InCl_3$ in presence of different concentrations of CA. Figure 2 a) to d) represents the cyclic voltammogram recorded onto FTO substrates with 0 M, 0.1 M, 0.3 M and 0.5 m of CA, respectively. The reduction peak of In is attributed around -0.77 V without CA. Upon increasing the CA in the electrolyte this peak shifts toward higher negative potentials from -0.77 V to -0.85 V, confirming the complex formation of $In^{3+}$ ions with CA by equation 3). Herrero and Ortega [38] have also reported the citrates are good complexing agents for the complex formation with $Cu^{2+}$ and $In^{3+}$.

$$In^{3+} + 3e^{-} \rightarrow In \qquad E_0 = -0.340 \text{ V versus NHE} \qquad \text{----------} \ (2)$$

### *3.2 Cyclic voltammetric study of* Cu-In *system*

The cyclic voltammograms obtained for Cu-In system recorded in presence of 0 M, 0.1 M, 0.3 M and 0.5 M CA are illustrated in figure 3 a) to d), respectively. At lower cathodic potential (~ -0.25 V), a small plateau region is observed (marked as ‘A’), which could be associated to the reduction of Cu, whereas, the region marked by B is likely due to reduction of In. The steep rise in cathodic current above -0.85 V could be due to the deposition of elemental In along with the over potential deposition of Cu. A plateau region observed in the range -0.75 V to -0.90 V could be suitable for the stoichiometric deposition of Cu-In alloy. It is observed that upon increasing the concentration of CA, the reduction peak associated to Cu has been systematically shifted towards higher cathodic potential (closer to In reduction potential). A broad plateau represents the Cu can be deposited for wide range. A role of CA is to reduce the mass transportation of copper by forming complex which could further support to deposit stoichiometric Cu-In layer. Well adherent and compact thin films of Cu-In were deposited at -0.85 V versus Ag/AgCl reference electrode, therefore the effect of concentrations of complexing agent is studied to the films deposited at -0.85 V.

### *3.3 Characterization of Cu-In layer*

The effect of CA on the structural properties of Cu-In alloy thin film was studied with the help of X-ray diffractometry. The x-ray diffraction (XRD) patterns of Cu-In layer grown at -0.85 V in presence of 0 M a), 0.1 M b), 0.3 M c) and 0.5 M d) CA are shown in figure 4. It has been observed that the layer deposited without CA (Fig. 4a) results only the deposition of copper with cubic crystal structure (JCPDF data, 85-1326). A layer deposited in presence of 0.1 M CA (Fig. 4b) exhibited several diffraction peaks, which are associated to Cu-In monoclinic crystal structure (JCPDF data, 35-1150). A peak associated to stable $Cu_{11}In_9$ compound was observed at 2θ ~ 42.17° (JCPDF data, 41-0883). It is noteworthy that the, metallic Cu and In related peak were not observed for a sample deposited in presence of 0.1 M CA. The film deposited in presence of 0.3 M CA, both CuIn and $Cu_{11}In_9$ phases were obtained with some metallic indium peaks. A higher concentration of CA, 0.5 M leads to the deposition of only metallic In of tetragonal structure (JCPDF data, 85-1409). Peaks related to the FTO substrate are marked as solid circle (●).

The surface morphology of Cu-In thin films was imaged with scanning electron microscope (SEM). Topographical SEM images of Cu-In layer deposited at -0.85 V in presence of different concentrations of CA are shown in the inset of figure 4. It can be clearly seen that the small spherical grains are deposited without CA, generally observed in metallic electrodeposition. It was further observed that the layers deposited without CA were powdery and poorly adherent to the substrate. On the contrary, the layers deposited in presence of CA were well adherent to the substrate with grayish metallic appearance. The clusters of size ranging from ~ 100 nm to over 1 micron are deposied with CA. Higher mass transport mechanism could be liable to enhance the particle size.

The compositional results obtained by EDAX for Cu-In thin films grown at -0.85 V with various concentrations CA are summarized in table 1. It is observed that without CA only Cu was present, whereas nearly stoichiometric Cu-In layers, (Cu/In ratio ~ 1) were deposited with 0.1 M CA. The higher concentration of CA, (0.3 M and 0.5 M) results In-rich samples with Cu/In ratio, 0.83 and 0.22, respectively. These results are in good agreement with XRD analyses discussed in earlier section.

### *3.4 Characterization of selenized Cu-In thin films*

Cu-In layers deposited at -0.85V in presence of various concentrations of CA were selenized in tubular furnace at rotary vacuum ~ 0.05 mbar in selenium ambient at 400 $^oC$ for 20 min. Figure 5 shows the XRD patterns of selenized Cu-In layers. Three most prominent reflections of tetragonal structure of CISe; (112), (204/220) and (312/116) are exhibited in the XRD spectrum of selenized Cu-In layer deposited with 0.1 M CA (Fig. 5a). However, the samples deposited with higher concentration of CA exhibit tetragonal structure of CISe along with secondary phases of $In_xSe_y$. Peaks appeared due to FTO are marked as solid circle (●).

The corresponding SEM images are given in the inset of figure 5. All the layers were compact and well adherent to the substrates. Large uniform grains of size ~ 500 nm can be clearly seen in Cu-In layer deposited in presence of 0.1 M CA. Mixed non-uniform spherical grains with small rods are formed upon selenization for the layer grown with 0.3 M CA. Upon selenization a large non-uniform clusters of size ~ 4 to 5 μm are clearly seen for the sample grown with 0.5 M CA could be due to the re-crystallization of material, which is desirable for the development of high efficiency solar cells.

The results obtained from UV-Vis spectroscopy, $(\alpha h\nu)^2$ versus $(h\nu)$ for selenized Cu-In layers deposited at -0.85 V with 0.1 M a), 0.3 M b) and 0.5 M c) CA are illustrated in figure 6. The value of energy band gap for stoichiometric CISe thin film deposited in presence of 0.1 M CA was estimated to be ~1.04 eV, which is in good agreement with the literature value [13]. The band gap was found to be increased systematically up to 1.19 eV upon increasing the concentration of CA, which is associated to the presence of $In_xSe_y$ and/or large grain size.

The compositional analysis obtained by EDAX of selenized Cu-In layers is summarized in table 1. Nearly stoichiometric CISe thin films with 25.2, 26.5 and 48.3 atomic percentage concentration of Cu, In and Se, respectively were deposited with 0.1 M CA in the electrolyte. The atomic percentage concentration of Cu and In was systematically decreased and increased, respectively upon increasing the molar concentration of CA. This is likely to be formation of complex with noble Cu elements. A systematic decrease of Cu/In ratio was observed in selenized Cu-In layers like pristine Cu-In thin films.

Current density-Voltage (J-V) characteristics of selenized Cu-In layers are illustrated in figure 7. The J-V characteristics of Cu-In layers prepared with 0.1 M CA is shown in the inset of figure 7. Au metal contacts of diameter 3 mm were made on FTO/ Cu-In and FTO/selenized Cu-In layer by thermal evaporation technique. As-deposited Cu-In layer showed ohmic behavior, whereas Mott-Schottky behavior was observed for selenized Cu-In samples. The value of the ideality factor (n) is calculated from the slope of straight line region of the forward bias by the following relation, [39].

$$n = \frac{q}{kT}\frac{dV}{d(\ln I)} ----------------------------- (3)$$

where 'q',V, n, k, T and I are the charge of electron, applied voltage, ideality factor, Boltzmann constant, temperature and diode current, respectively. The values of ideality factor 1.93, 2.10 and 2.26 were calculated for CISe layers deposited with 0.1 M, 0.3 M and 0.5 M CA, respectively. The ideality factor calculated for the sample deposited with 0.1 M is low, due to the less tunneling through barrier and likely less defects present within the material.

Figure 8 represent the Photoresponse curve (Photocurrent density verses time) for standard n-type Silicon a), p-type Silicon b), selenized Cu-In layers deposited at -0.85 V with 0.1 M c), 0.3 M d) and 0.5 M e) CA. 1 M KCl solution was used with chopped white light of intensity 10 mW/cm$^2$. The photocurrent  in PEC process is originated from the minority charge carriers, therefore, the direction of observed photocurrent gives the type of majority charge carries. The standard p-type and n-type Si of resistivity, 0.05 Ω cm was used as a reference. The photocurrent measured for n-type Si upon illumination was found to be increased along the positive direction (fig. 8a), whereas, the photocurrent was found to be increased along negative direction for p-type Si (fig. 8b). The photocurrent measured for selenized Cu-In layers electrodeposited with 0.3 M (fig. 8d) and 0.5 M (fig. 8e) was increased towards positive direction, indicates the n-type conductivity due to the higher contents of In. The growth of n-type conductive CISe layer is tudied in detail by Persson et. al. [40]. The photocurrent measured for selenized Cu-In layers with 0.1 M (fig. 8c) was found to be increased towards negative direction confirms the p-type conductivity. With negative bias an electrons from the conduction band are extracted, therefore the current response is limited for p-type semiconductor [41]. However, upon illumination of higher energy than the bandgap, electrons are promoted from the valence band to the conduction band and driven to the solid/electrolyte interface and finally transferred to the solution by reduction of the $H^+$ ions, enhancing the cathodic current response [42-43]. This effect can be clearly seen in the figure 8b) and c) where the cathodic current is higher under illumination, which confirms the p-type conductivity of the layer. The sharp edges observed at ON and OFF of the light are associated to the growth of less defective CISe layers, which is suitable for the development of high efficiency solar cells.

The Raman spectra of selenized Cu-In layers grown with various concentrations of CA are depicted in figure 9. The highest intensity peak exhibited in all spectra about 170 cm$^{-1}$ is associated to A1 mode of the chalcopyrite CISe. The small peaks attributed around 207 cm$^{-1}$ and 224 cm$^{-1}$ corresponding to E and B2 mode of CISe [44]. The peak observed at 260 cm$^{-1}$ in figure 9 (a) is associated to the Cu-Se phase. The intensity of this peak was found to be decreased upon increasing the content of CA in a bath. These results are again in good agreement with the earlier results. A similar change (decrease) in the intensity of the Cu-Se peak is reported by Park et al. [45]. A small shoulder observed about 152 cm$^{-1}$ in figure 9 c) is associated to the formation of ordered defect compound (ODC) of the CISe phase [46]. The peak appeared around 116 $cm^{-1}$ corresponds to the calibration of Raman wave numbers [47].

### *3.4 Solar cell characteristics*

A superstrate configuration FTO/CdS/selenized Cu-In /Au was prepared to study the solar cell properties. Cu-In layer was electrodeposited at -0.85 V with 0.1 M CA and selenized in tubular furnace at 400 $^{o}$C for 20 min. Dark and illuminated (AM 1.5, 100 mW/$cm^2$) J-V characteristics were measured using solar stimulator. CdS/CISe layer was etched in NaCN solution to remove the leftover selenium traces and/or other secondary oxides/compounds formed during the selenization. A typical dark and illuminated J-V, curve are depicted in figure 10 (a) and (b), respectively.

The solar cell parameters, open circuit voltage ($V_{OC}$), short circuit current ($J_{SC}$), fill factor (FF) and power conversion efficiency η, were measured to be 493 mV, 20 mA/$cm^2$, 43 % and 4.05 %, respectively. The measured efficiency is comparatively low, however which could be further improved with optimization of surface treatment conditions.

The J-V characteristics of a thin film solar cell (TFSC) can be described by simple diode equation, [48]

$$J = J_o exp\left[\frac{q}{nkT}(V - R_S J)\right] + GV - J_L \ldots\ldots\ldots\ldots\ldots\ldots\ldots\ldots\ldots\ldots\ldots\ldots\ldots\ldots .. (4)$$

where, J and V is the current density and applied bias voltage, $J_o$ is the reverse saturation current density, $J_L$ is the photocurrent density, $R_s$ is the series resistance and G is the shunt conductance.

The plot of dV/dJ against 1/J and dV/d(J+$J_{SC}$) against 1/(J+$J_{SC}$) under dark and illumination for the case $R_sG<<1$ is shown in figure 11 (a) and 11 (b), respectively.

The values of the series resistances 7.42 Ω-$cm^2$ and 0.94 Ω-$cm^2$ for dark and illuminated condition were obtained from the intercept to y- axis. The values of shunt conductance (G) were extracted from dJ/dV versus V, figure 12 a) and 12 b) for dark and illuminated condition, respectively. G values were obtained from the minimum value of the slope dJ/dV in reverse bias. Shunt conductance of the device in dark and illuminated condition were 1.01 mS/$cm^2$ and 10.25 mS/$cm^2$, respectively. For an efficient photovoltaic device the shunt conductance has to be as small as possible. Smaller value of G represents the less internal leakage through the cell. The calculated values of $R_S$ and G are listed in table 2.

## 4.0 CONCLUSIONS

The role of CA on the properties of electrodeposited Cu-In layer was studied. The reduction potential of Cu was found to be shifted towards higher cathodic potential upon increasing the CA in the bath. A poorly adherent, powdery Cu layer was deposited without CA. Well adhesive, polycrystalline and stoichiometric Cu-In layers were obtained at -0.85 V with 0.1 M CA. Upon selenization the Cu-In layers prepared with 0.1 M CA possesses polycrystalline CISe with tetragonal structure without secondary phases. The large clusters of size over a micron were observed upon selenization. The values of optical band-gap were estimated in the range of 1.05 eV to 1.18 eV for selenized Cu-In layers deposited in various concentrations of CA. Ohmic behavior was observed for stoichiometric Cu-In layer, whereas Mott-Schottky nature was exhibited in the selenized Cu-In layers. PEC studies revealed that the CISe layer grown with 0.1 M CA were p-type and 0.3 M and 0.5 M CA deposits n-type conductivity. The formation of chalcopyrite CISe for all selenized Cu-In was confirmed by Raman analyses. The Raman peaks associated to Cu-Se were attributed in CISe layer deposited with 0.1 M CA, whereas ODC phase of CISe were formed in CISe layer prepared with 0.3 and 0.5 M CA. Solar cell device fabricated with selenized Cu-In layer prepared at -0.85 V with 0.1 M CA measured an efficiency ~ 4.05 % under 100 mW/cm$^2$. The values of $R_s$, 7.42 Ω-cm$^2$, 0.94 Ω-cm$^2$ and G, 1.01 mS/cm$^2$ 10.25 mS/cm$^2$ were calculated under dark and illuminated condition, respectively.

## ACKNOWLEDGEMENT

The authors wish to acknowledge Defence Research and Development Organization (DRDO), New Delhi and Department of Science and Technology (SERI) for financial support. ABR is thankful to CSIR for Senior Research Fellowship.

## REFERENCES

[1] A. N. Tiwari, D. K. Pandya, K. L. Chopra, Fabrication and analysis of all-sprayed $CuInS_2$/ZnO solar cells, Solar Cells 22 (1987) 263-273.

[2] M. G. Lakhe, N. B. Chaure, Characterization of electrochemicallydeposited $CuInTe_2$ thin films for solar cell applications, Sol. Energy Mater. Solar Cells 123 (2014) 122-129.

[3] M. Gloeckler, J.R. Sites, Band-gap grading in Cu(In,Ga)$Se_2$ solar cells, J. Phys. Chem. of Solids 66 (2005) 1891–1894

[4] A. Antony, A. S. Asha, R Yoosuf, R. Manoj, M. K. Jayras, Growth of $CuInS_2$ thin films by sulphurisation of Cu–In alloys, Sol. Energy Mater. Solar Cells 81 (2004) 407-417.

[5] T. Nakada, A. Kunioka, Direct evidence of Cd diffusion into $Cu(In,Ga)Se_2$ thin films during chemical-bath deposition process of CdS films, Appl. Phys. Lett. 74 (1999) 2444-2446.

[6] A. M. Hermanna, C. Gonzaleza, P. A. Ramakrishnan, D. Balzar, N. Popa, P. Rice, C. H. Marshall, J. N. Hilfiker, T. Tiwald., P.J. Sebastian, M.E. Calixto, R.N. Bhattacharya, Fundamental studies on large area $Cu(In,Ga)Se_2$ films for high efficiency solar cells, Sol. Energy Mater. Solar Cells 70 (2001) 345-361.

[7] C. R. Abernathy, C. W. Bates, A. A. Anani, B. Haba, G. Smestad, Production of single phase chalcopyrite $CuInSe_2$ by spray pyrolysis, Appl. Phys. Lett. 45 (1984) 890-892.

[8] Z. Baji, Z. Lábadia, G. Molnár, B. Pecz, A.L. Toth, J. Toth, A. Csik, I. Bársony, Post-selenization of stacked precursor layers for CIGS, Vacuum 92 (2013) 44-51.

[9] Z. Yu, L. Liu, Y. Yan, Y. Zhang, S. Li, C. Yan, Y. Zhang, Y. Zhao, Properties of different temperature annealed $Cu(In,Ga)Se_2$ and $Cu(In,Ga)_2Se_{3.5}$ films prepared by RF sputtering, Appl. Surf. Sci. 261 (2012) 353-359.

[10] M. Chandramohana, S. Velumani, T. Venkatachalam, Experimental and theoretical investigations of structural and optical properties of CIGS thin films, Mater. Sci. Eng. B 174 (2010) 205-208.

[11] A. B. Rohom, P. U. Londhe, N. B. Chaure, The effect of pH and selenization on the properties of $CuInSe_2$ thin films prepared by electrodeposition technique for device Applications, J. Solid State Electrochem. 19 (2014) 201–210.

[12] M. A. Green, K. Emery, Y. Hishikawa, W. Warta and E. D. Dunlop, Solar cell efficiency tables (version 45), Prog. Photovolt. Res. Appl. 23 (2015) 1-9.

[13] N. B. Chaure, J. Young, A. P. Samantilleke, I. M. Dharmadasa, Electrodeposition of n-i-p-type $CuInSe_2$ multilayers for photovoltaic application, Sol. Energy Mater. Solar Cells 81 (2004) 125-133.

[14] N. B. Chaure, A. P. Samantillleke, R. P. Burton, J. Young, I. M. Dharmadasa, Electrodeposition of p+, p, i, n and n+-type copper indium gallium diselenide for development of multilayer thin film solar cells, Thin Solid Films 472 (2005) 212-216.

[15] Priyanka U. Londhe, Ashwini B. Rohom and Nandu B. Chaure, $CuInSe_2$ thin film solar cells prepared by low-cost electrodeposition techniques from a non-aqueous bath, RSC Adv. 5 (2015) 89635 -89643.

[16] R. N. Bhattacharya, J. F. Hiltner, W. Batchelor, M. A. Contreras, R. N. Noufi, J. R. Sites, 15.4% $CuIn_{1-x}Ga_xSe_2$-based photovoltaic cells from solution-based precursor films, Thin solid Films 361-362 (2000) 396-399.

[17] B. Lee, S. L. Park, J. Lee, J. Jeong, J. Kim, C. Chung, and D. Lee, ACS Applied Materials & Interfaces 8 (2016) 24585.

[18] R. Koutsikou, M. Bouroushian, Pulse potential electrodeposition of (112)-textured chalcopyrite $CuInSe_2$ films from acidic aqueous solutions, Electrochim. Acta 178 (2015) 856–870.

[19] R.N. Bhattacharya, Solution Growth and Electrodeposited $CuInSe_2$Thin Films, J. Electrochem. Soc. 130 (1983) 2040-2042.

[20] R. Ugarte, R. Schrebler, R. Cordova, E. A. Dalchiele, H. Gomez, Electrodeposition of CuInSe2 thin films in a glycine acid medium, Thin Solid Films 340 (2000) 117–124.

[21] F. J. Pern, J. Goral, R.J. Matson, T.A. Gessert, R. Noufi, Device quality thin films of $CuInSe_2$ by a one-step electrodeposition process, Solar Cells 24 (1988) 81.

[22] M. G. Ganchev, K. D. Kochev, Investigation of the electrodeposition process in the Cu-In-Se System, Sol. Energy Mater. Solar Cells 31 (1993) 163-170.

[23] J. Yuan, C. Shao, L. Zheng, M. Fan, H. Lu, C. Hao, D. Tao, Fabrication of CuInS2 thin film by electrodeposition of Cu-In alloy, Vacuum 99 (2014) 196-203.

[24] M. E. Calixto, P. J. Sebastian, $CuInSe_2$ thin films formed by selenization of Cu–In precursors, J. Mater. Sci. 33 (1998) 339-345.

[25] T. P. Gujar, V. R. Shinde, J. W. Park, H. K. Lee, K. D. Jung, O. S. Joo, Electrochemical Approach for Selenization of Stacked Cu-In Layers for Formation of Crystalline $CuInSe_2$, J. Electrochem. Soc. 155 (2008) E131-E135.

[26] D. Pottier, G. Maurin, Preparation of polycrystalline thin films of $CuInSe_2$ by electrodeposition, J. Appl. Electrochem. 19 (1989) 361.

[27] L. Thouin, S. Rouquette-Sanchez, J. Vedal, 10th Europ. Photovoltaic Solar Energy Conf., Lisbon, 1991, 893.

[28] P. Luo, C. Zhu, G. Jiang, Preparation of $CuInSe_2$ thin films by pulsed laser deposition the Cu–In alloy precursor and vacuum selenization, Solid State Comm. 146 ( 2008) 57-60.

[29] P. P. Prosini, M. L. Addonizio, A. Antonaia, S. Loreti, Effect of substrate surface treatment on the nucleation and crystal growth of electrodeposited copper and copper–indium alloys, Thin Solid Films 298 (1996) 191-196.

[30] J. Herrero, J. Ortega, Electrodeposition of Cu-In alloys for preparing $CuInS_2$ thin films, Sol. Energy Mater. Solar Cells 20 (1990) 53-65.

[31] Y. Cummings, G. Zoppi, I. Forbes, D. Colombara, L. M. Peter, F. Marken, Rocking disc electro-deposition of CuIn alloys, selenisation, and pinhole effect minimisation in CISe solar absorber layers, Electrochim. Acta 79 (2012)141-147.

[32] S. H. Liu, F. S. Chen, C. H. Lu, Synthesis of $CuInSe_2$ films via selenizing the Cu-In alloy-containing nanopowders,, J. Alloy. Comp. 517 (2012) 14–19.

[33] G. Norsworthy, CR Eidholm, A. Halaj, V. K. Kapur, R. Roe, B. M Basol, R. Matson, CIS film growth by metallic ink coating and Selenization, Sol. Energy Mater. Solar Cells 60 (2000) 127.

[34] C. Kind, C. Feldmann, A. Quintilla, E. Ahiswede, Citrate-Capped $Cu_{11}In_9$ Nanoparticles and Its Use for Thin-Film Manufacturing of CIS Solar Cells, Chem. Mater. 23 (2011) 5269-5274.

[35] N. B. Chaure , S. Bordas , A. P. Samantilleke , S. N. Chaure , J. Haigh , I. M. Dharmadasa, Investigation of electronic quality of chemical bath deposited cadmium sulphide layers used in thin film photovoltaic solar cells, Thin Solid Films, 2003, 437, 10–17.

[36] Y. Lai, F. Liu, Z. Zhang, J. Liu, Y. Li, S. Kung, J. Li, Y. Liu, Cyclic voltammetry study of electrodeposition of $Cu(In,Ga)Se_2$ thin films, Electrochim. Acta 54 (2009) 3004-3010.

[37] J. Liu, F. Liu, Y. Lai, Z. Zhang, J. Li and Y. Liu, Effect of sodium sulfamate on electrodeposition of $CuInGaSe_2$ thin film, J. Electroanal. Chem., 651 (2011) 191-196

[38] J. Herrero and J. Ortega, Electrodeposition of cu-ln alloys for preparing $CulnS_2$ thin films, Solar Energy Mater. 20 (1990) 53-65

[39] S. M. Sze, K. K. Ng, Physics of Semiconductor Devices, IIIrd edn. (Wiley, New York, 2007) 170-171.

[40] C. Persson, Y. J. Zhao, S. Lany, and A. Zunger, n-type doping of CuInSe2 and CuGaSe2, Physical Review, 72 (2005) 035211

[41] R. Memming, Semiconductor Electrochemistry, Wiley-VCH, Weinheim, (2001) 167.

[42] C. Guillen, J. Herrero, Structure, morphology and photoelectrochemical activity of $CuInSe_2$ thin films as determined by the characteristics of evaporated metallic precursors, Sol. Energy Mater. Sol. Cells 73 (2002) 141-149.

[43] F. Caballero-Briones, A. Palacios-Padrós, F. Sanz, $CuInSe_2$ films prepared by three step pulsed electrodeposition. Deposition mechanisms, optical and photoelectrochemical studies, Electrochim. Acta, 56 (2011) 9556-9567.

[44] A. Chao, S. Ahn, J. H. Yun, J. G. Wak, S. K. Ahn, K. Shin, H. Song, K. H. Yoon, Non-vacuum processed $CuInSe_2$ thin films fabricated with a hybrid ink, Sol. Energy Mater. Sol. Cells 109 (2013) 17-25.

[45] J. H. Park, I. S. Yang, Micro-Raman spectroscopy in polycrystalline $CuInSe_2$ formation, Appl. Phys. A 58 (1994) 125-128.

[46] O. Ramadani, J. F. Gulliemoles, D. Loncot, P. P. Grand, E. Chassing, O. Kerrac, E. Rzepka, One-step electrodeposited $CuInSe_2$ thin films studied by Raman spectroscopy, Thin Solid Films, 515 (2007) 5909-5912.

[47] M. Klose, R. Schaffler, Gert Irmer, Michael Brieger, D. Schmid, Hans W. Schock, Raman scattering investigations of $CuInSe_2$ films deposited by coevaporation and laser ablation, Proc. SPIE 2403 (1995) doi:10.1117/12.206254.

[48] S. S. Hegedus and W. N. Shafarman, Thin-Film Solar Cells Device Measurements and Analysis, Prog. Photovolt: Res. Appl. 12 (2004) 155-176

## Table Captions

**Table 1.** A summary of the compositional analysis of as-prepared and selenized Cu-In layers electrodeposited at -0.85 V in presence of different concentrations of CA.

**Table 2.** Solar cell parameters obtained from selenized Cu-In layer (CISe) under dark and illuminated conditions.

## Figure Captions

**Figure 1.** Cyclic voltammograms recorded in Cu precursor solution with 0 M a), 0.1 M b), 0.3 M c) and 0.5 M d) CA. The measurement were performed at scan rate of 5 mV/sec without agitation at working temperature 45 $^{o}$C.

**Figure 2.** Cyclic voltammograms recorded in $InCl_3$ solution in presence of 0 M a), 0.1 M b), 0.3 M c) and 0.5 M d) CA. The measurements were performed at temperature 45 $^{0}$C without agitation with scan rate 5 mV/sec.

**Figure 3.** Cyclic voltammograms recorded for Cu-In alloythin film in presence of 0 M a), 0.1 M b), 0.3 M c) and 0.5 M d) CA in 3 mM $CuCl_2$ and 6 mM $InCl_3$ precursor solutions. The measurements were performed with scan rate 5 mV/sec at 45 $^{0}$C without agitation.

**Figure 4.** XRD patterns of Cu-In layers electrodeposited at -0.85 V in presence of 0 M a), 0.1 M b), 0.3 M c) and 0.5 M d) CA. Corresponding SEM images are shown in the inset.

**Figure 5.** XRD patterns of the selenized Cu-In layers electrodeposited at – 0.85V in presence of 0.1 M a), 0.3 M b) and 0.5 M c) CA. Reflection associated to FTO and $In_xSe_y$ are marked as (•) and (*), respectively. Inset shows the corresponding SEM micrographs.

**Figure 6.** The plots of $(\alpha h\nu)^2$ versus $(h\nu)$ of the selenized Cu-In layer electrodeposited at – 0.85V in presence of 0.1 M a), 0.3 M b) and 0.5 M c) CA.

**Figure 7.** Semilogarithmic graphs of ln (I) versus applied bias of selenized Cu-In layers electrodeposited at -0.85V in presence of 0.1 M a), 0.3 M b) and 0.5 M c) CA. The J-V characteristics of Cu-In layer prepared with 0.1 M CA is shown in inset.

**Figure 8.** Photoresponse curves, photocurrent density verses time for standard n-type Silicon a), p-type Silicon b), selenized Cu-In layers deposited with 0.1 M c), 0.3 M d) and 0.5 M e) CA.

**Figure 9.** Raman spectra for selenized Cu-In layers deposited with 0.1 M a), 0.3 M b) and 0.5 M c) CA.

**Figure 10.** A typical dark a) and illuminated b) current density-voltage characteristics measured for superstrate configuration consisting glass/FTO/CdS/selenized Cu-In layer/Au.

**Figure 11.** A plot of dV/dJ versus 1/(J) a) and dV/d(J+$J_{SC}$) versus 1/(J+$J_{SC}$) b) for glass/FTO/CdS/selenized Cu-In layer/Au solar cell device measured under dark and illumination, respectively.

**Figure 12.** A plot of dJ/dV versus V a) and d/(J+$J_{SC}$)/dV versus V b) for glass/FTO/CdS/selenized Cu-In layer/Au solar cell measured under dark and illumination, respectively.

**Table 1.**

| CA Concentration in (M) | Elemental Composition (At %) | | | | | | |
|---|---|---|---|---|---|---|---|
| | Cu-In **layers** | | | **Selenized Cu-In layer (CISe)** | | | |
| | **Cu** | **In** | **Cu/In** | **Cu** | **In** | **Se** | **Cu/In** |
| **0** | 100 | 0 | - | - | - | - | - |
| **0.1** | 49.2 | 50.8 | 0.97 | 25.2 | 26.5 | 48.3 | 0.95 |
| **0.3** | 45.4 | 54.6 | 0.83 | 17.5 | 29.4 | 53.1 | 0.60 |
| **0.5** | 18.2 | 81.8 | 0.22 | 10.4 | 32.7 | 56.9 | 0.32 |

**Table 2.**

| Solar cell device | $V_{OC}$ (mV) | $J_{SC}$ (mA/cm$^2$) | FF | η % | G (dark) (mS/cm$^2$) | G (ill) (mS/cm$^2$) | $R_S$ (dark) Ω cm$^2$ | $R_S$ (ill) Ω cm$^2$ |
|---|---|---|---|---|---|---|---|---|
| **Glass/FTO /CdS/selenized- Cu-In /Au** | 493 | 20 | 0.41 | 4.05 | 1.01 | 10.25 | 7.42 | 0.94 |

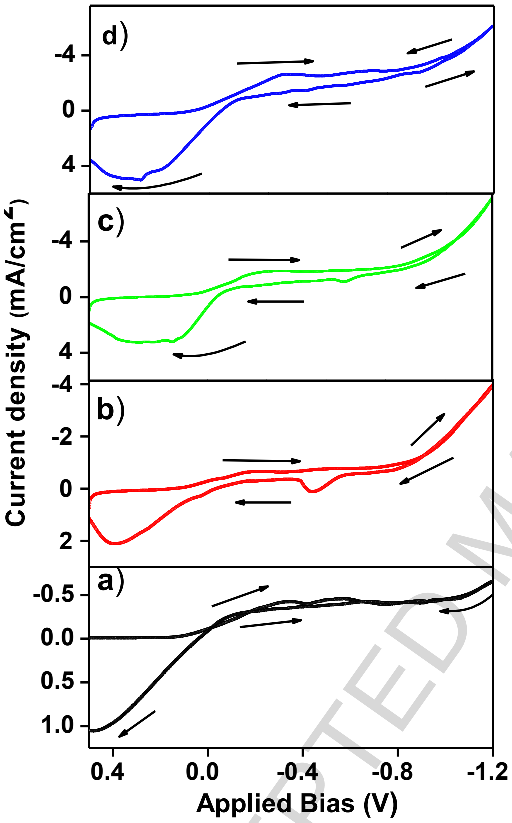
d)
-4
0
4
c)
-4
0
4
b)
-4
-2
0
2
a)
-0.5
0.0
0.5
1.0
0.4
0.0
-0.4
-0.8
-1.2
Applied Bias (V)
Current density (mA/cm²)

**Figure 1**

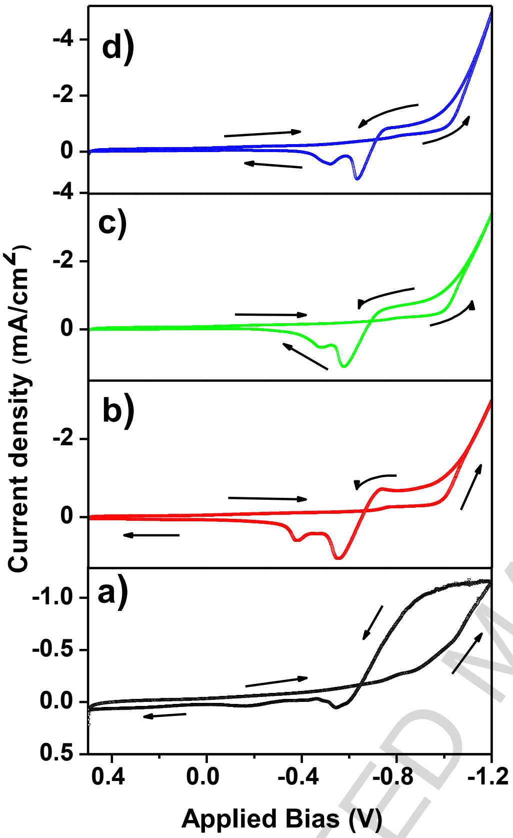
d)
c)
b)
a)
-4
-2
0
-4
-2
0
-2
0
-1.0
-0.5
0.0
0.5
Current density (mA/cm$^2$)
0.4
0.0
-0.4
-0.8
-1.2
Applied Bias (V)

Figure 2

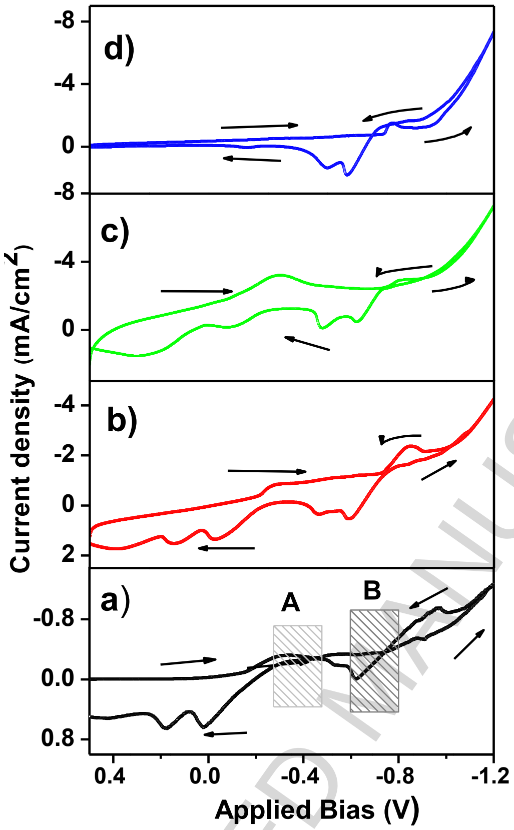
d)
c)
b)
a)
A
B
-8
-4
0
-8
-4
0
-4
-2
0
2
-0.8
0.0
0.8
Current density (mA/cm$^2$)
0.4
0.0
-0.4
-0.8
-1.2
Applied Bias (V)

**Figure 3**

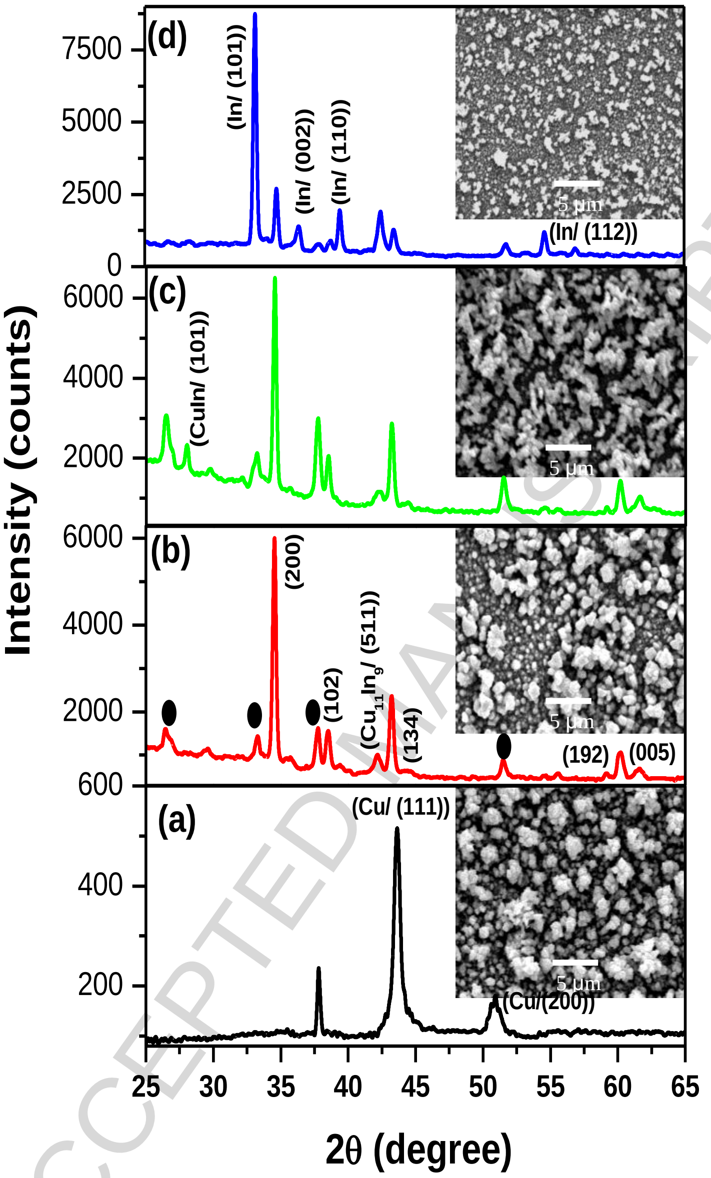
(d)
(In/ (101))
(In/ (002))
(In/ (110))
(In/ (112))
5 µm
(c)
(CuIn/ (101))
5 µm
(b)
(200)
(102)
(Cu$_{11}$In$_9$/ (511))
(134)
(192)
(005)
5 µm
(a)
(Cu/ (111))
(Cu/(200))
5 µm
7500
5000
2500
0
6000
4000
2000
6000
4000
2000
600
600
400
200
Intensity (counts)
25
30
35
40
45
50
55
60
65
2θ (degree)

**Figure 4**

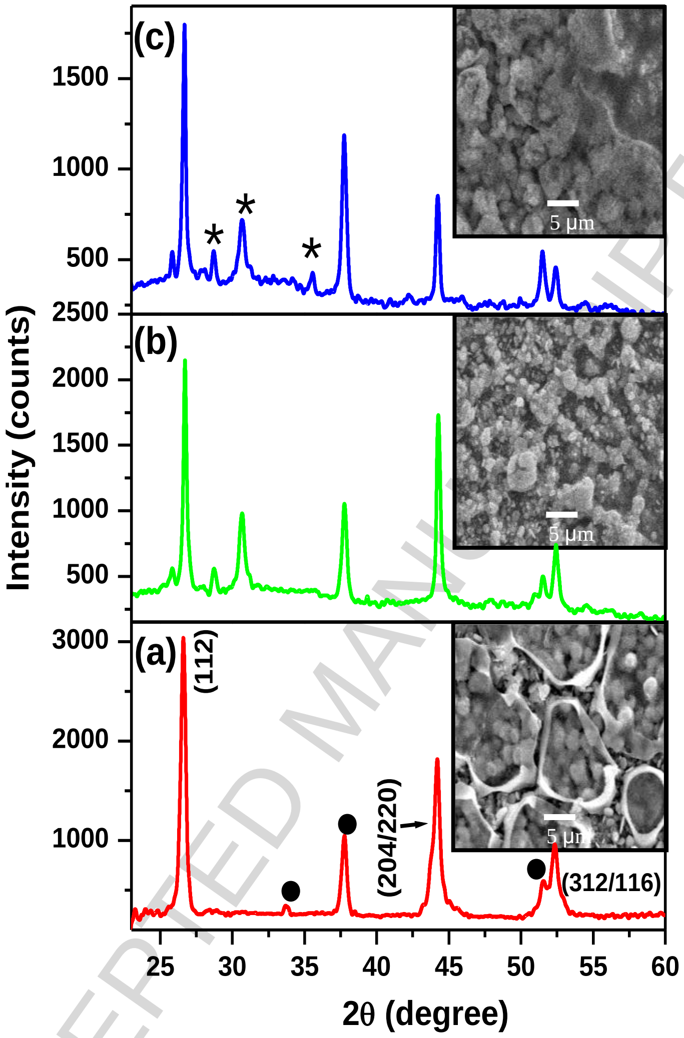
(c)
(b)
(a)
*
*
*
5 μm
5 μm
5 μm
(112)
(204/220)
(312/116)
Intensity (counts)
2θ (degree)
1500
1000
500
2500
2000
1500
1000
500
3000
2000
1000
25
30
35
40
45
50
55
60

Figure 5

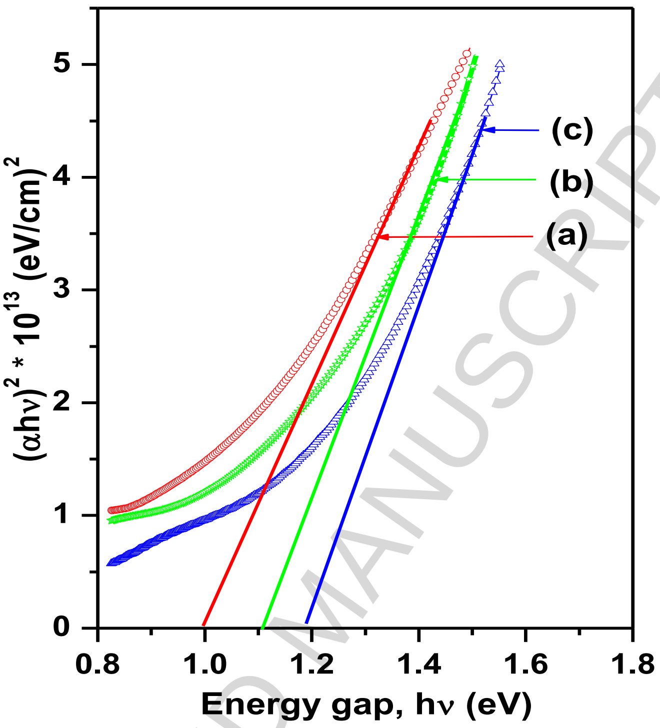
$(\alpha h\nu)^2 * 10^{13}$ (eV/cm)$^2$
Energy gap, hν (eV)
0
1
2
3
4
5
0.8
1.0
1.2
1.4
1.6
1.8
(c)
(b)
(a)

Figure 6

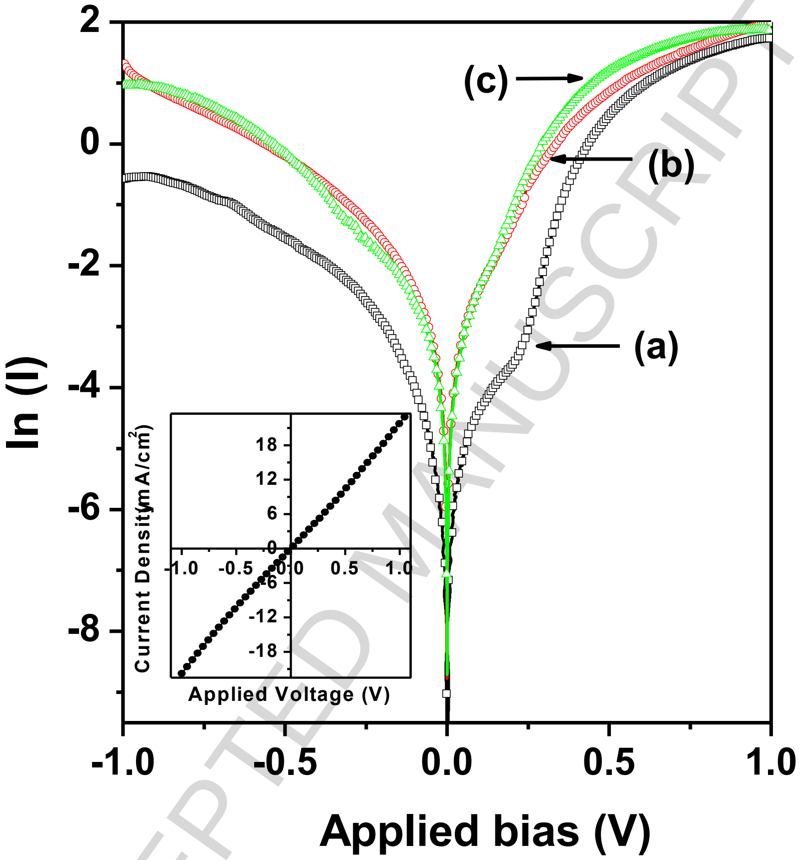
ln (I)
Applied bias (V)
2
0
-2
-4
-6
-8
-1.0
-0.5
0.0
0.5
1.0
(a)
(b)
(c)
Current Density (mA/cm$^2$)
Applied Voltage (V)
18
12
6
0
-6
-12
-18
-1.0
-0.5
0.0
0.5
1.0

Figure 7

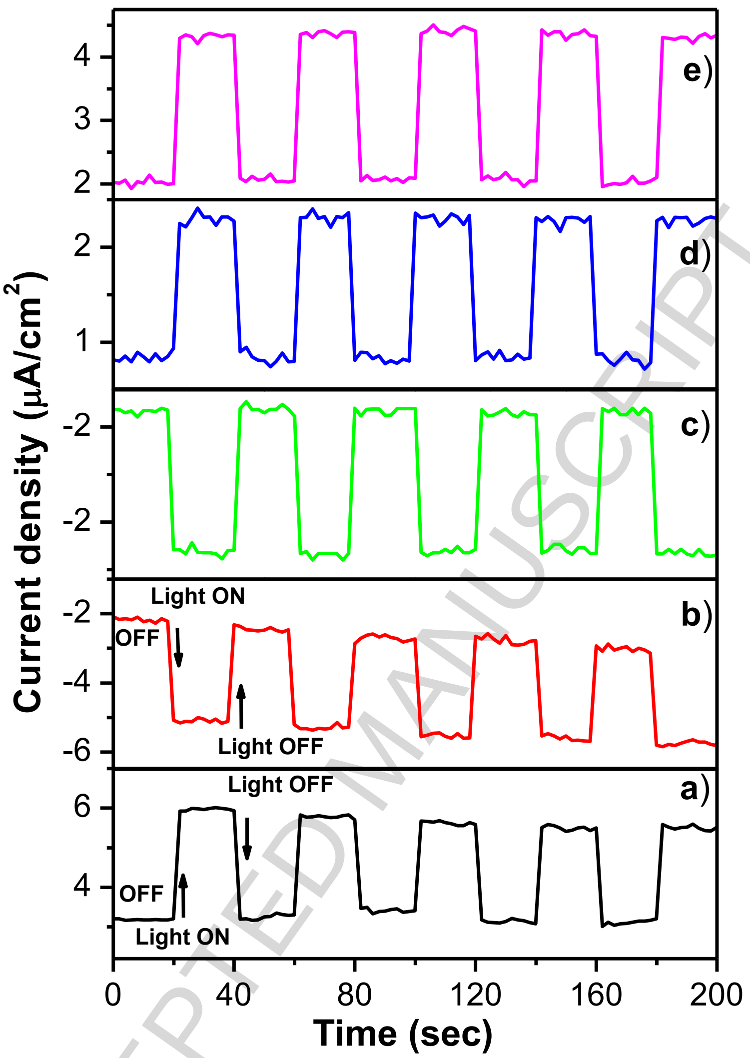
Current density (µA/cm$^2$)
Time (sec)
0
40
80
120
160
200
e)
d)
c)
b)
a)
4
3
2
2
1
-2
-2
-2
-4
-6
6
4
Light ON
OFF
Light OFF
Light OFF
OFF
Light ON

**Figure 8**

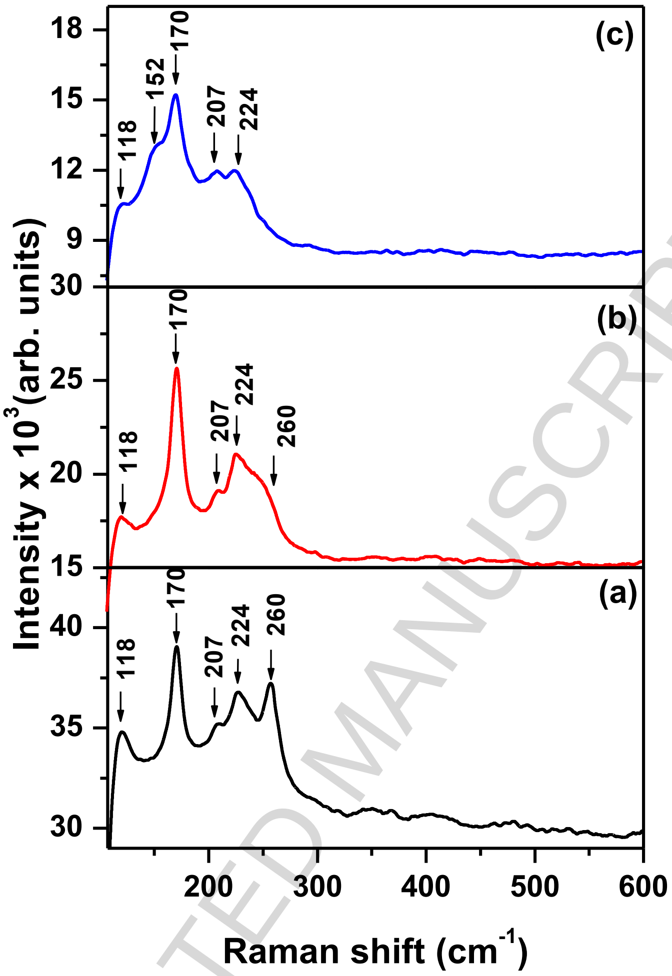

(c)
(b)
(a)
118
152
170
207
224
260
18
15
12
9
30
25
20
15
40
35
30
Intensity x 10$^3$(arb. units)
200
300
400
500
600
Raman shift (cm$^{-1}$)

**Figure 9**

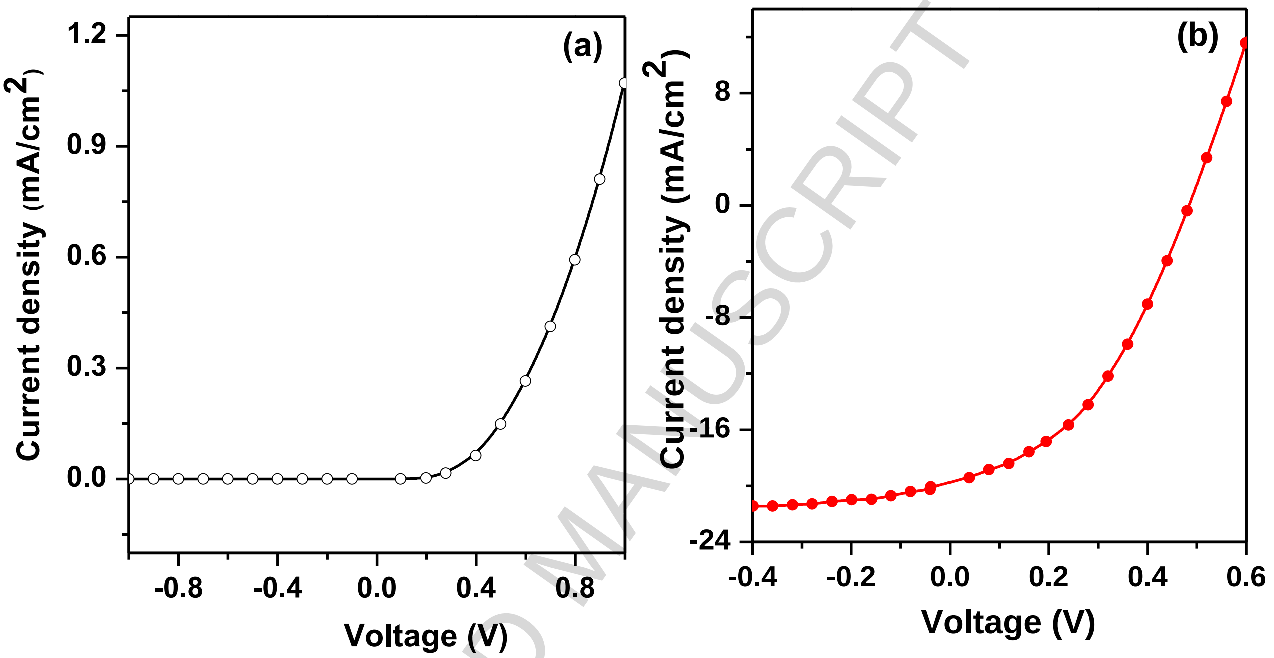
(a)
Current density (mA/cm$^2$)
1.2
0.9
0.6
0.3
0.0
-0.8
-0.4
0.0
0.4
0.8
Voltage (V)
(b)
Current density (mA/cm$^2$)
8
0
-8
-16
-24
-0.4
-0.2
0.0
0.2
0.4
0.6
Voltage (V)

**Figure 10**

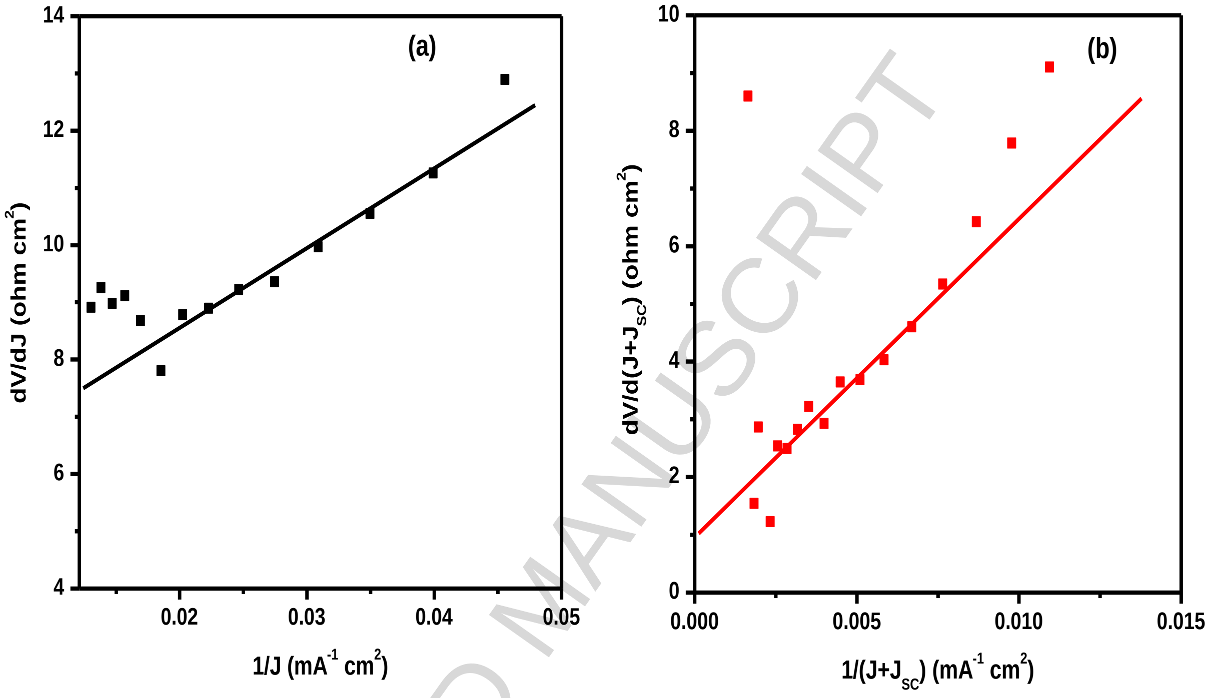
(a)
dV/dJ (ohm cm$^2$)
1/J (mA$^{-1}$ cm$^2$)
14
12
10
8
6
4
0.02
0.03
0.04
0.05
(b)
dV/d(J+J$_{SC}$) (ohm cm$^2$)
1/(J+J$_{SC}$) (mA$^{-1}$ cm$^2$)
10
8
6
4
2
0
0.000
0.005
0.010
0.015

**Figure 11**

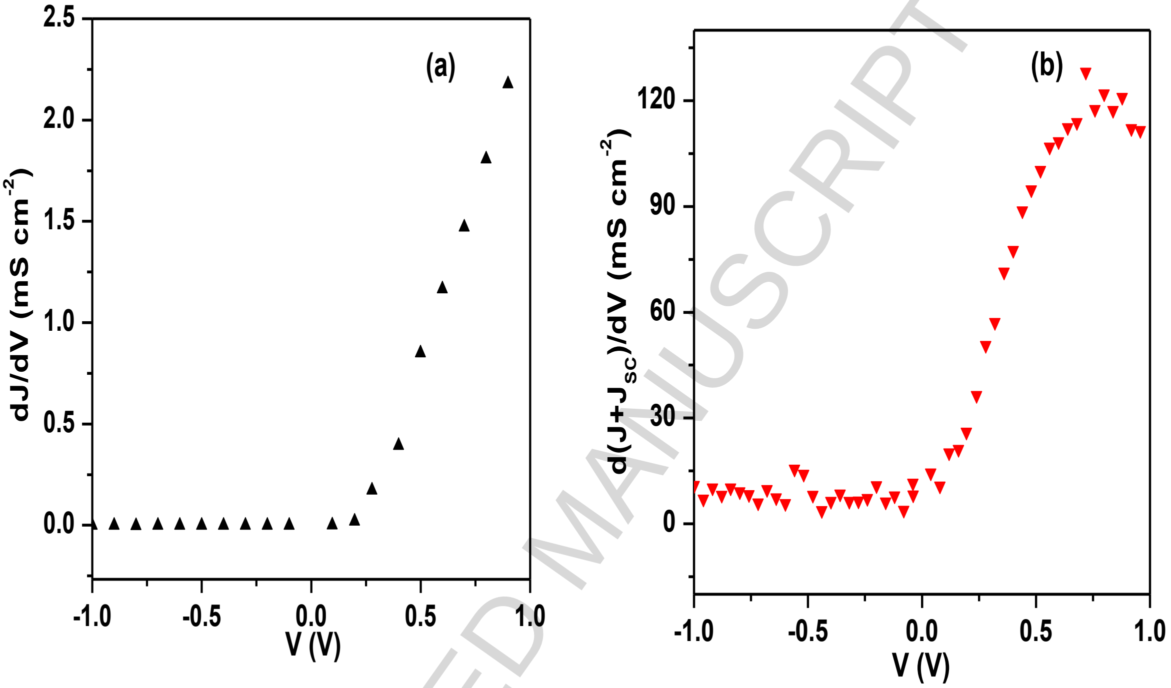
(a)
dJ/dV (mS cm$^{-2}$)
2.5
2.0
1.5
1.0
0.5
0.0
-1.0
-0.5
0.0
0.5
1.0
V (V)
(b)
d(J+J$_{SC}$)/dV (mS cm$^{-2}$)
120
90
60
30
0
-1.0
-0.5
0.0
0.5
1.0
V (V)

Figure 12

## Research highlights

- Citric acid plays an important role to control the electrodeposition of Cu-In Layers.
- Polycrystalline and stoichiometric CISe layers are prepared via two stage process.
- p and n-type conductivity CISe layers can be prepared by two stage processing technique.
- Selenized Cu-In solar cell measured over 4 % power conversion efficiency.